

Electronic and magnetic properties of transition-metal doped ScN for spintronics applications

Fares Benissad and Abdeslem Houari*

*Theoretical Physics Laboratory, Department of Physics,
University of Bejaia, Bejaia, Algeria*

(Dated: September 23, 2020)

Abstract

Motivated by the ongoing interest in nitrides as materials for spintronics applications we have studied effects of doping with magnetic transition-metal elements ($T=\text{Cr, Mn, Fe, Co}$ and Ni) on the electronic properties of semiconducting scandium nitride. Using density functional together with the generalized gradient approximation (GGA) as well as PBE0r hybrid functional (with different mixing of the exact exchange), two different doping amounts 25% ($\text{Sc}_{0.75}\text{T}_{0.25}\text{N}$) and 10% ($\text{Sc}_{0.9}\text{T}_{0.1}\text{N}$) have been investigated. This is done in comparison to the reference compound ScN with a strong focus on identifying candidates for half-metallic or semiconducting ferromagnetic ground states. Within GGA, only $\text{Sc}_{0.75}\text{Cr}_{0.25}\text{N}$ and $\text{Sc}_{0.75}\text{Mn}_{0.25}\text{N}$ are found to be semiconducting and half-metallic, respectively. The use of hybrid functional changes drastically these finding, where $\text{Sc}_{0.75}\text{Fe}(\text{Co, Ni})_{0.25}\text{N}$ become half-metals and $\text{Sc}_{0.75}\text{Cr}(\text{Mn})_{0.25}\text{N}$ are found both semiconductors. However, additional calculations assuming antiferromagnetic ordering revealed that $\text{Sc}_{0.75}\text{Cr}_{0.25}\text{N}$ is the only compound of this series, which prefers an antiferromagnetic (and semiconducting) ground state. For the lower concentration, $\text{Sc}_{0.9}\text{T}_{0.1}\text{N}$, similar results have been predicted, and all the doped nitrides are found to prefer ferromagnetic ground state over an antiferromagnetic one.

* corresponding author: abdeslam.houari@univ-bejaia.dz

I. INTRODUCTION

The simultaneous exploitation of the charge and spin degrees of freedom of electronic materials is at the heart of the rapidly emerging field of spintronics. Of particular interest in this field are especially two types of materials classes, namely, dilute magnetic semiconductors (DMS) and half-metallic ferromagnets (HMF) [1, 2] with the latter being regarded as good candidates for spin injection in magneto-electronic devices [3].

Specifically, Mn-doped III-V semiconducting nitrides and arsenides such as (Ga,Al,In)(N,As) have been extensively investigated [4, 5]. However, their use in practical applications is hampered by their rather low Curie temperatures. So far, the highest Curie temperature of about 173 K was reported for Mn-doped GaN [6, 7]. Yet, it has been argued that ferromagnetism above even 300 K could be possible in N-rich growth of Ga(Mn)N [8]. Further obstacles to applications are the known low solubilities of the magnetic ions in the semiconductor matrix due to the different crystal structures assumed by the metallic dopants. Finally, spin injection is often affected by the resistivity mismatches at semiconductor-ferromagnet interfaces [9, 13]

In contrast, transition-metal (TM) nitride semiconductors and their alloys recommend themselves due to their exceptional optical, electro-mechanical, and magnetic properties, which make them promising candidates for applications in optoelectronic devices [9, 14–17].

Scandium nitride ScN crystallizes in the rocksalt structure with a lattice parameter of 4.50 Å [18, 19]. It has an indirect band gap of ~ 0.9 eV [20–23]. ScN has been experimentally investigated by a variety of techniques [24–27]. In addition, *ab initio* calculations have been carried out to investigate its electronic structure [28–30, 33–35], confirming the experimental results as the rocksalt crystal structure and lattice constant. While some DFT-based calculations using the local density approximation found ScN as a semi-metal [28–32], More elaborated calculations using the framework of the *GW* approximation succeeded to reproduce the experimental band gap of ~ 0.9 eV [33–36].

Considerable effort was devoted to tailoring the physical properties of ScN through non-magnetic doping [21]. However, only few experimental studies have been reported on dilute ferromagnetism in doped ScN [37–40]. Al-Brithen *et al.* incorporated Mn atoms to obtain $\text{Sc}_{1-x}\text{Mn}_x\text{N}$ type alloys with $0 \leq x \leq 0.25$, crystallizing in a tetragonal structure [37]. Electronic and optical properties of Sc(Mn)N thin films were also investigated, with up to

11% doping [38]. The authors suggested that dilute manganese doping compensates for the high n -type carrier concentrations, and an n -type to p -type carrier type transition could be observed. However, the magnetic properties of these films were not studied. Insertion of a low amount of iron (Fe) atoms in ScN has been achieved by Constantin *et al.* [39], who gave a magnetic moment of $\sim 0.037 \mu_B/\text{Fe atom}$ at the experimental volume of the pristine system.

On the theoretical side, structural and optical properties of $\text{Cr}_{1-x}\text{Sc}_x\text{N}$ alloys have been studied together with Cr-doped GaN [12]. However, with respect to the magnetic properties, focus was on the latter material. Supercell calculations on Mn-doped ScN have been carried out to study trends of the magnetic properties [9–11, 44]. It was found that the exchange interactions are long range and affected by disorder and carrier concentrations [10, 11]. Furthermore, a structural phase transition has been predicted in $\text{Mn}_x\text{Sc}_{1-x}\text{N}$ from a zinc-blende phase to a hexagonal phase [11]. For iron doping, $\text{Fe}_{0.25}\text{Sc}_{0.75}\text{N}$ has been investigated by means of DFT calculations, which predicted a magnetic semiconductor [40]. The study, however, has focused more on the transport and thermoelectric properties.

Recently, a DFT-based study using the GGA+ U method has been reported on a large series of transition-metal doped (T,Sc)N (with T=Ti, V, Cr, Mn, Fe, Co and Ni)[45]. The occurrence of half-metallicity was predicted for V-, Cr-, and Mn-doping, whereas metallic behavior was expected for doping with late transition-metal atoms.

Extending a previous study on pure ScN and $\text{Sc}_{0.75}\text{Mn}_{0.25}\text{N}$ as based on the GGA [44], we investigate in the present investigation ScN doped with a larger variety of transition metal including Cr, Mn, Fe, Co, and Ni). In doing so, we go beyond previous studies by applying a hybrid-functional approach in addition to GGA calculations.

II. THEORY AND COMPUTATIONAL METHOD

The first principles calculations of the present work are based on density functional theory (DFT) [46, 47]. In a first step, exchange-correlation effects are accounted for by the generalized gradient approximation (GGA) [48]. In addition, we applied a hybrid functional approach, which as well known replaces part of the exchange functional of the GGA by the exact exchange term provided by the Hartree-Fock method [49, 50]. Within this general approach, several implementations are in use. While the PBE0 method includes the exact

exchange with a fraction of 25% in all space [51], the HSE06 method uses this fraction only for the short-range part while keeping the long-range part of the exchange interaction at the GGA level [52]. This idea is put to its extreme by the PBE0r functional, which restricts the exact exchange interaction to onsite matrix elements in a local orbital basis [53, 54]. The accuracy of the PBE0r functional, with respect to experiment, has been demonstrated in a study of transition-metal oxides [55]. Furthermore, a very recent extensive benchmark investigation using HSE06 as well as PBE0r functionals has been reported [56], where the latter is found to have an accuracy in the same range of the former. The PBE0r method is also used in the present study, where the exact exchange contribution is considered with different fractions (see below in **IIIB**). Notice that a small value of 5% suffices to reproduce the experimentally reported ScN band gap of 0.9 eV.

The electronic and magnetic properties were calculated using the CP-PAW code, which is the original implementation of the Projector Augmented Wave (PAW) method [57]. It uses the Car-Parrinello *ab initio* molecular dynamics (AIMD) framework to simultaneously calculate the atomic structure and the electronic wave functions [58]. The Mermin functional [59] was applied to treat variable occupations of the one-electron energy eigenstates, allowing to describe correctly metallic systems.

Total energy convergence was assumed when the difference between two successive iterations was less than 10^{-5} Hartree. The plane-wave cutoff was 40 Hartree and the Brillouin-zone integrations were performed on a $(6 \times 6 \times 6)$ mesh (leading to 260 k-points in the Brillouin-zone) using the linear tetrahedron method [60, 61] with Blöchl correction [62]. The convergence with respect to plane waves expansion as well as k-points, has been carried out carefully by increasing the cutoff value until an accuracy of (i.e the variation of the total energy is less than) 10^{-5} Hartree is reached. Full description of the calculations details can be found in our recent publication [63]. In addition, all structural parameters have been optimized. The relaxed atomic positions (geometry optimization) and the electronic ground state are obtained efficiently using a friction, within the Car-Parrinello molecular dynamics method. The lattice constant corresponding to theoretical equilibrium, is optimized by an isotropic expansions and contractions.

III. RESULTS AND DISCUSSIONS

A. Electronic structure of pure ScN

Since the electronic properties of ScN are well established both experimentally and theoretically, this section just serves as a reference for the subsequent discussion. More thorough description can be found in literature, as mentioned above in the introduction. The equilibrium structure of pure ScN has been determined by minimization of the total energy versus unit cell volume using both the GGA and hybrid functionals. From this, lattice constants of 4.58 Å and 4.52 Å were obtained from the GGA and the hybrid-functional calculations, respectively. While the former as expected is somewhat larger than the experimental value of 4.50 Å, the latter shows better agreement.

The site- and orbital-projected densities of states as calculated using the GGA, within the experimental lattice, is displayed in Fig. 1. they confirm the semiconducting state with

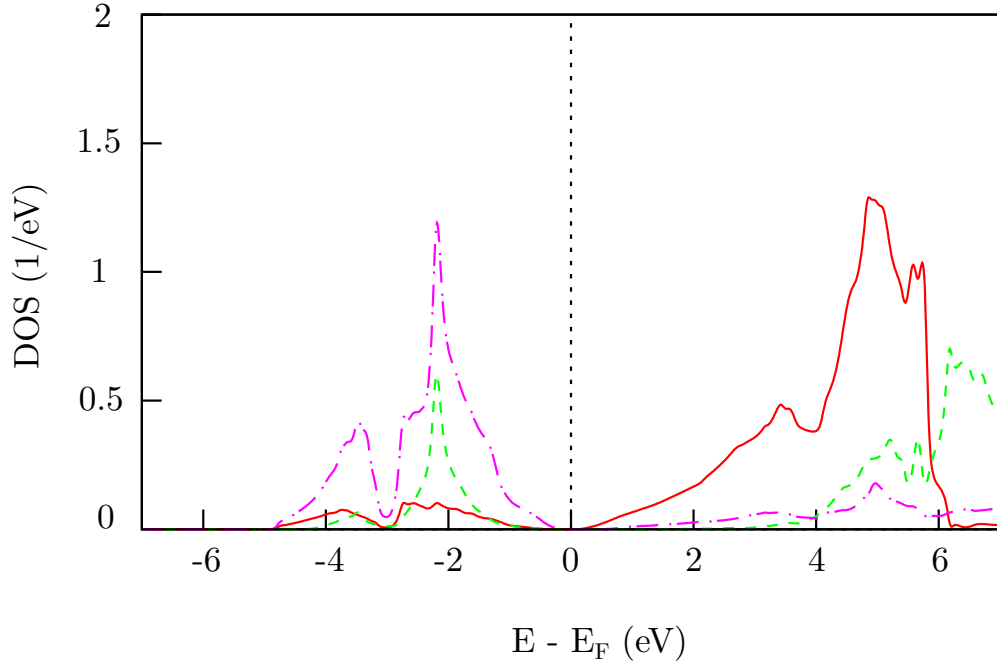


FIG. 1. (Color online) Site- and orbital projected densities of states (DOS) of ScN. Sc- d t_{2g} , Sc- d e_g , and N p contributions as given in red (solid), green (dashed), and magenta (dash-dotted), respectively.

a band gap of about 0.35 eV, which is much smaller than the measured experimental one

(~ 0.9 eV). This is due to the well-known failure of the local and semi-local approximations to reproduce experimental band gaps. Since many previous LDA and GGA calculations have predicted vanishing gap, as pointed out in the introduction[31, 32], we have performed additional complementary GGA with a another method based on a different wavefunction basis set. Using the full-potential augmented spherical wave method (FP-ASW) [42, 43], with a carefully converged calculation, a band gap of 0.38 eV has been computed. Still being far from the experimental one, this result is close to our first one.

While the nitrogen $2p$ -states are more prevailing in the valence band, the conduction band is dominated by the transition-metal d states. The latter fall into non-bonding t_{2g} sub-bands in the lower part (with a large peak around 5 eV), whereas the e_g states due to stronger overlap with the N- $2p$ and, hence, larger splitting into bonding and anti-bonding manifolds are found at higher energies. As already reported, the trivalent character of Sc is almost complete, i.e. ScN can be written as $\text{Sc}^{+\delta}\text{N}^{-\delta}$ with $\delta \simeq 3$, making the compound almost ionic [44].

In a second step, hybrid-functional calculations were performed with a 5%-admixture of the exact exchange interaction as mentioned above, which allowed to reproduce the experimentally observed band gap of 0.9 eV.

B. Trends of electronic structure and magnetic properties of $\text{Sc}_{1-x}\text{T}_x\text{N}$ (T=Cr, Mn, Fe, Co, Ni)

This section is devoted to the study the effect of the substitution of scandium by several transition metal atoms, i.e. $\text{Sc}_{1-x}\text{T}_x\text{N}$, where T=Cr, Mn, Fe, Co, and Ni, with two different $x=0.25$ and $x=0.10$ concentrations.

In the first case, the simulations are performed using a simple-cubic supercell of the fcc-rocksalt structure of the form $\text{Sc}_3\text{T}_1\text{N}_4$. The calculated theoretical equilibrium lattice parameters are found very close to each others in the whole series. With hybrid functional framework, we computed the following values: 4.423 Å (T=Cr), 4.439 Å (T=Mn), 4.457 Å (T=Fe), 4.430 Å (T=Co) and 4.445 Å (T=Ni), whereas those calculated by GGA are about 3% larger. Thus, the substitution leads a slightly smaller lattice constants compared to pure ScN. We mention, however, that neither experimental nor theoretical data are available in literature, to which our results could be compared.

We have first considered a ferromagnetic alignment of the transition metal atoms. The ferromagnetic state is found more stable than the spin-degenerate situation for all five dopants considered here. The electronic densities of states of the five compounds as described within the GGA framework are shown in Fig. 2. Obviously, all types of substitution lead to loss of the semiconducting character of pure ScN. While Mn, Fe, Co, and Ni insertion induce metallic behavior, $\text{Sc}_{0.75}\text{Cr}_{0.25}\text{N}$ is found to be a half-metal. In the latter case, an energy band gap of $\sim 0.9\text{ eV}$ is opened in the spin-down states, whereas a small contribution to the density of states at the Fermi level can be seen in the spin-up states. Hence, the compound is at the verge of being a semiconductor. Similarly, $\text{Sc}_{0.75}\text{Mn}_{0.25}\text{N}$ is close to being half-metallic.

In all the compounds, the distribution of the scandium d -states remains almost unchanged to that in pure ScN indicating only weak hybridization with the d states of the dopant. In contrast, the d states of the substitutional alloying elements can be regarded as in-gap states between N- p and Sc- d states of ScN.

In $\text{Sc}_{0.75}\text{Cr}_{0.25}\text{N}$ and $\text{Sc}_{0.75}\text{Mn}_{0.25}\text{N}$ the non-bonding d - t_{2g} states of chromium and manganese experience a strong exchange splitting. As a result, spin-majority states are completely filled leading to a high-spin configuration of the Cr and Mn t_{2g} shells. However, the two compounds differ with respect to the d - e_g states. Like in ScN, the dopant d - e_g states hybridize strongly with the N- p states and are split into bonding and anti-bonding manifolds below and above the Fermi energy, respectively. While in the case of Cr the latter are empty for both spin populations, the Mn- d - e_g states are only half-filled. As a result, magnetic moments per Cr and Mn atom of $2.9\mu_B$ and $3.8\mu_B$, respectively, were obtained in the doped compounds.

Beyond Cr and Mn, the exchange splitting of the t_{2g} states decreases progressively due to the filling of the corresponding minority-spin states, which are shifted below the Fermi level. Finally, for $\text{Sc}_{0.75}\text{Ni}_{0.25}\text{N}$ the exchange splitting is almost vanishing and both the majority and minority spin channels of the Ni- t_{2g} states are completely filled. The calculated magnetic moments per dopant atom are $2.8\mu_B$, $1.7\mu_B$, and $0.2\mu_B$ for the Fe-, Co-, and Ni-doped compounds, respectively.

Since the main purpose of this investigation is the search for ferromagnetic half-metals and semiconductors, a correct evaluation of the band gap is of great importance. As mentioned above, use of the hybrid functional allowed to obtain the experimentally reported band

gap for ScN. In order to explore the effect of the main ingredient of the hybrid functional scheme which is the inclusion of the exact exchange, we have performed calculations with three different mixing parameters (i.e the weight of the Fock term, noted α). The PBE0r functional allows to specify this mixing parameter on each site. So, we kept the one on Sc and N atoms fixed to 5% (or $\alpha = 0.05$, like in pure ScN), while increasing the one on the transition metal element gradually: 5% ($\alpha = 0.05$), 10% ($\alpha = 0.10$) and finally 20% ($\alpha = 0.20$). The corresponding results of the site- orbital-, and spin-projected densities of states for the five doped compounds are displayed in Fig. 3.

In Fig. 3-(a) corresponding to the lowest value of the mixing parameter ($\alpha = 0.05$), the electronic structure of $\text{Sc}_{0.75}(\text{Fe, Co, Ni})_{0.25}\text{N}$ doped nitrides remains almost unchanged, with respect to GGA, and still shows metallic character. The situation is different for the doping with Cr and Mn. Specifically, for $\text{Sc}_{0.75}\text{Cr}_{0.25}\text{N}$ a ferromagnetic semiconducting is found with a band gap of ~ 0.5 eV, whereas $\text{Sc}_{0.75}\text{Mn}_{0.25}\text{N}$ turns out to be a ferromagnetic half-metal with a finite DOS in the majority-spin channel and a band gap of ~ 0.8 eV in the minority-spin channel.

When increasing the the mixing parameter to $\alpha = 0.1$, the picture start to change noticeably, as shown in Fig. 3-(b). Here, while the electronic character of two first $\text{Sc}_{0.75}\text{Cr}(\text{Mn})_{0.25}\text{N}$ compounds remains the same as for $\alpha = 0.05$ (just with a slightly enhanced gap fo the Cr-doped nitride ~ 0.7 eV), we notice that $\text{Sc}_{0.75}\text{Fe}(\text{Co})_{0.25}\text{N}$ turn to be half-metallic ferromagnets with a small minority spin band gap. Moreover, Ni-doped nitride $\text{Sc}_{0.75}\text{Ni}_{0.25}\text{N}$ is found at the verge of being a half-metal too, where a tiny gap starts to open in the minority spin channel. This situation becomes completely resolved with the highest mixing parameter value $\alpha = 0.2$, leading to a clear semiconducting ferromagnetism in the two first compounds $\text{Sc}_{0.75}\text{Cr}(\text{Mn})_{0.25}\text{N}$, (with band gap values of ~ 0.85 and ~ 0.45 , for Cr and Mn doping, respectively). In the other Fe-, Co- and Ni-doped nitrides, a very net half-metallic character is stabilized. Of course, both physical states are of high interest for spintronics applications.

Overall, the trend of the densities of states of all the compounds is very similar to the one observed for the GGA calculations, for the three mixing parameters, especially concerning the Sc and N electronic DOS. In particular, the projected DOS given in Figs. 2 and 3 have almost the same shape and distribution and the general discussion of the GGA results applies also to the hybrid-functional calculations apart from the relative shifts of the groups

of bands. There is, however, a noticeable difference concerning the exchange splitting of t_{2g} and e_g shells in the transition metal ions, when increasing the weight of the Fock term α . This can be seen from the computed values of the magnetic moments for the different cases, as shown in Tab. I. A saturated magnetic moments for all the compounds are obtained with the two last fractions of the exact exchange (i.e $\alpha = 0.1$ to $\alpha = 0.2$), where semiconducting or half-metallic behavior are obtained. For the lowest value $\alpha = 0.05$, however, the metallic character of Fe-, Co- and Ni-doped nitrides leads to non-integer magnetic moments. Hence, as expected, the hybrid-functional approach favors a high-spin configuration as compared to the GGA. We notice that within both frameworks the total magnetic moment per unit cell arises almost exclusively from the dopant atom. This is the case in all five compounds, where the N atom is found to carry a moment of less than $0.1 \mu_B$.

According to the densities of states of Fig. 3, the magnetic moments of all doped compounds arise almost completely from the t_{2g} states (visible from the exchange splitting between the two spin populations), except the Co- and Ni-doped ones. In the latter, in particular, a small contribution from e_g states is visible. This is a consequence of the weak hybridization of these states with the nitrogen p -states, whereas the e_g states due to their strong bonds with the nitrogen states and the resulting large bonding-antibonding splitting showing very similar spin-up and spin-down contributions.

TABLE I. Calculated magnetic moments, in μ_B , of the transition metal elements within GGA as well as hybrid functionals.

| Sc _{0.75} T _{0.25} N | GGA | Hyb. Func | | |
|--|-----|-----------------|----------------|----------------|
| | | $\alpha = 0.05$ | $\alpha = 0.1$ | $\alpha = 0.2$ |
| T = Cr | 2.9 | 3 | 3 | 3 |
| T = Mn | 3.8 | 4 | 4 | 2 |
| T = Fe | 2.8 | 3.5 | 3 | 3 |
| T = Co | 1.7 | 1.9 | 2 | 2 |
| T = Ni | 0.2 | 0.85 | 1 | 1 |

The particular case of Sc_{0.75}Fe_{0.25}N has been studied by Sharma *et al.* using the modified Becke-Johnson local-density approximation (mBJ-LDA) [41]. They have found that the p - d hybridization between iron and nitrogen states gives rise to a magnetic semiconductor, which

is in contradiction with our results, that is a metallic character predicted from GGA and half-metallic one with hybrid-functional calculations.

Very recently, Sukkabot *et al.* using the GGA+ U method with a U value of 3.9 eV for all the compounds have investigated ScN doped with several transition elements [45]. They found half-metallic ferromagnetism in both Mn- and Cr-doped ScN. While the former result is in agreement with our study with a low admixture of exact exchange ($\alpha = 0.05$), we predict in contrast that Cr-doped ScN is a semiconductor, as well as Mn-doped one with larger mixing parameter.

To finalize the investigation of $\text{Sc}_{0.75}\text{T}_{0.25}\text{N}$ compounds, the calculations of the ferromagnetic states were complemented by investigations regarding possible antiferromagnetic alignment of the magnetic moments of the dopant atoms. To this end, supercells (formed by doubled simple-cubic cell) were considered to simulate a simple type I antiferromagnetic alignment (AFM<001>). The latter consists on a ferromagnetic plans alternating along the z-axis direction. To the best of our knowledge, the study of AFM ordering in doped-ScN has not been reported elsewhere.

As a result, except for chromium doped ScN antiferromagnetic order was found to be less stable than the ferromagnetic state discussed above. Specifically, in $\text{Sc}_{0.75}\text{Cr}_{0.25}\text{N}$ the Cr atoms prefer to antiferromagnetic over ferromagnetic one, which is by ~ 8 mHa and ~ 10 mHa per formula unit higher in energy, in GGA and hybrid functional, respectively. The site-, orbital, and spin-projected densities of states of antiferromagnetic $\text{Sc}_{0.75}\text{Cr}_{0.25}\text{N}$ are shown in Fig. 4. The GGA calculations lead to a metallic state with an almost vanishing density at Fermi level and magnetic moments of $\pm 2.75 \mu_{\text{B}}$ located at the Cr ions. In contrast, use of the hybrid functional gives rise to a semiconducting state with a band gap of ~ 0.8 eV, and a slightly enhanced Cr magnetic moment of $\pm 2.8 \mu_{\text{B}}$.

The second part of our study consists to investigate the electronic structure and magnetic properties of the doped-ScN nitride with a lower substitution concentration, that is $\text{Sc}_{0.9}\text{T}_{0.1}\text{N}$ ordered compounds (T=Cr, Mn, Fe, Co and Ni). Like in the previous case, we started first by considering a ferromagnetic alignment of the transition metal ions. The obtained densities of states within GGA are shown along side with those obtained with hybrid functional frameworks in Fig.5. Here, we show the results of moderate ($\alpha = 0.1$) and highest ($\alpha = 0.2$) mixing parameters, and we omit the lowest one ($\alpha = 0.05$) since it does not bring noticeable changes to the GGA findings.

While GGA describes all the compounds as metals, the hybrid functional predicts both semiconducting and half-metallic ferromagnetic characters. Let us first notice that the densities of N and Sc atoms are nearly not affected with respect to pure ScN, where the states of the former dominate the valence band and those of the latter are prevailing in the conduction band. In GGA (Fig. 5-a), the transition metal t_{2g} states experience an exchange splitting of the two spin populations due to the weak bonding with nitrogen, which decreases in intensity going from Cr to Ni. In contrast, the e_g states with a strong hybridization with N states show similar spin-up and spin-down distributions. The hybrid functional with a mixing parameter of $\alpha = 0.1$ leads to a half-metallicity in Cr-, Mn-, Fe- and Ni-doped nitrides; whereas the Co-doped one still behaves as a metal. When increasing the parameter to $\alpha = 0.2$, some changes occur and we find a similar situation to the high concentration ($x=0.25$) compounds. Thus, Cr- and Mn-doping lead to semiconducting nitrides, while $\text{Sc}_{0.9}\text{Fe}(\text{Co}, \text{Ni})_{0.1}\text{N}$ ones become half-metals. We notice that the overall trends of the transition metal densities of states and the contribution to the magnetic moments are also similar to the high concentration case.

Finally, we complemented this second part of the study by a check on the possible stability of antiferromagnetic alignment of the transition metal ions (AFM $\langle 001 \rangle$, as in the first case of high concentration). Here, and in contrast to the former case, all the $\text{Sc}_{0.9}\text{T}_{0.1}\text{N}$ doped nitrides are found energetically more stable in the ferromagnetic configuration.

IV. SUMMARY AND CONCLUSION

To conclude, first-principles calculations as based on density functional theory were used to explore the change in electronic and magnetic behavior of ScN upon substitution with transition-metal ions $\text{T}=\text{Cr}, \text{Mn}, \text{Fe}, \text{Co}, \text{and Ni}$, i.e. $\text{Sc}_{1-x}\text{Cr}_x\text{N}$, with two concentrations $x=0.25$ and $x=0.1$. In particular, the influence of exchange effects beyond the semi-local approximation as captured by the generalized gradient approximation was investigated.

In a first step, the electronic structure of ScN was studied by both GGA and hybrid-functional calculations to establish a reference for the doped compounds. With a fraction as small as 5% of the exact exchange functional the experimental band gap of ScN of 0.9 eV could be reproduced.

Within GGA approximation, and initially focusing on the ferromagnetic state, we found $\text{Sc}_{0.75}\text{T}_{0.25}\text{N}$ to be ferromagnetic metals for $\text{T} = \text{Mn}, \text{Fe}, \text{Co}, \text{and Ni}$; whereas $\text{Sc}_{0.75}\text{Cr}_{0.25}\text{N}$

is a half-metal. Decreasing the substitution concentration to 10%, all $\text{Sc}_{0.9}\text{T}_{0.1}\text{N}$ compounds are found metallic. Using hybrid-functional framework, with increasing exact exchange mixing parameter, the electronic behavior of the compounds changes progressively. As a consequence, $\text{Sc}_{0.75}\text{T}_{0.25}\text{N}$ are established as ferromagnetic half-metals for $\text{T} = \text{Fe}, \text{Co}, \text{and Ni}$, while both $\text{Sc}_{0.75}\text{Cr}(\text{Mn})_{0.25}\text{N}$ are turned out to be semiconducting ferromagnets. Similar findings have been obtained in second substitution concentration $\text{Sc}_{0.9}\text{T}_{0.1}\text{N}$.

Considering antiferromagnetic ordering, it was found unstable for all $\text{Sc}_{0.75}\text{T}_{0.25}\text{N}$ compounds except $\text{Sc}_{0.75}\text{Cr}_{0.25}\text{N}$, leading to a semiconducting antiferromagnetic ground state of this compound. In the lower concentration, however, all $\text{Sc}_{0.9}\text{T}_{0.1}\text{N}$ are found to prefer a ferromagnetic ground state.

We conclude that in the two limits of substitution concentrations, the predicted physical properties could be interesting for practical applications in spintronics.

ACKNOWLEDGMENTS

The authors gratefully acknowledge V. Eyert for a critical reading of the manuscript and fruitful discussions. A. H. also acknowledges P. E. Blöchl for providing his CP-PAW code.

-
- [1] M. Bowen, M. Bibes, M. A. Barthélémy, J. P. Contour, A. Anane, Y. Lemaitre, and A. Fert, Appl. Phys. Lett. **82**, 233 (2003).
 - [2] S. A. Wolf, D. D. Awschalom, R. A. Buhrman, J. M. Daughton, S. von Molnar, M. L. Roukes, A. Y. Chtchelkanova, and D. M. Treger, Science **294**, 1488 (2001).
 - [3] C. M. Fang, G. A. De Wijs, and R. A. De Groot, J. App. Phys. **91**, 8340 (2002).
 - [4] S. Sonoda, S. Shimizu, T. Sasaki, Y. Yamamoto, and H. Hori J. Crys. Growth **237**, 1358 (2002).
 - [5] K. M. Yu, W. Walukiewicz, T. Wojtowicz, W. L. Lim, X. Liu, Y. Sasaki, M. Dobrowolska, and J. K. Furdyna, Appl. Phys. Lett. **81**, 844 (2002).
 - [6] K.Y. Wang, R. P. Champion, K. W. Edmonds, M. Sawicki, T. Dietl, C. T. Foxon, and B. L. Gallagher, AIP Conf. Proc. **772**, 333 (2005).
 - [7] T. Jungwirth, K. Y. Wang, J. Masek, K. W. Edmonds, J. König, J. Sinova, M. Polini,

- N. A. Goncharuk, A. H. MacDonald, M. Sawicki, A. W. Rushforth, R. P. Campion, L. X. Zhao, C. T. Foxon, and B. L. Gallagher, *Phys. Rev. B* **72**, 165204 (2005).
- [8] M. B. Haider, C. Constantin, H. Al-Britthen, G. Caruntu, C. J. OConner, and A. R. Smith, *physica status solidi (a)* **202**, 1135 (2005).
- [9] A. Herwadkar and W. R. L. Lambrecht, *Phys. Rev. B* **72**, 235207 (2005).
- [10] A. Herwadkar, W. R. L. Lambrecht, and M. Van Schilfgaarde, *Phys. Rev. B* **77**, 134433 (2008).
- [11] A. Alsaad, M. Bani-Yassein, I.A. Qattan, A. Ahmad, and S.R. Malkawi, *Physica. B* **405**, 1408 (2010).
- [12] A. Alsaad, *Physica. B* **405**, 951 (2010).
- [13] G. Schmidt, D. Ferrand, L. W. Molenkamp, A. T. Filip, and B. J. Van Wess, *Phys. Rev. B* **62**, R4790 (2000).
- [14] A. Houari, S. F. Matar, M. A. Belkhir, and M. Nakhl, *Phys. Rev. B* **75**, 064420 (2007).
- [15] A. Houari, S.F. Matar, and M. A. Belkhir, *J. Magn. Magn. Mat.* **322**, 392 (2008).
- [16] A. Houari, S. F. Matar, and V. Eyert *Phys. Rev. B* **82**, 241201(R) (2010).
- [17] V. Rajan, L. Bellaiche, and E. J. Walter, *Phys. Rev. Lett.* **90**, 257602 (2003).
- [18] D. Gall, I. Petrov, N. Hellgren, L. Hultman, J. E. Sundgren, and J. E. Greene, *J. Appl. Phys.* **84**, 6034 (1998).
- [19] T. D. Moustakas, R. J. Molnar, and J. P. Dismukes, *Electrochem. Soc. Proc.* **96**, 197 (1996).
- [20] H. A. Al-Britthen, and A. R. Smith, *Appl. Phys. Lett.* **77**, 2485 (2000).
- [21] H. A. Al-Britthen, A.R. Smith, and D. Gall, *Phys. Rev. B* **70**, 045303 (2004).
- [22] P. Burmistrova, J. Maassen, T. Favaloro, B. Saha, S. Salamat, Y. R. Koh, M. Lundstrom, A. Shakouri, and T. D. Sands, *J. Appl. Phys.* **113**, 153704 (2013).
- [23] G. Conibeer, *Mater. Today* **10**, 42 (2007).
- [24] G. V. Naik, B. Saha, T. D. Sands, and A. Boltasseva, 4th International Topical Meeting on Nanophotonics and Metamaterials (NANOMETA 2013), Seefeld, Austria, 2-6 January, 2013.
- [25] H. A. Al-Britthen, E. M. Trifan, D. C. Ingram, A. R. Smith, and D.Gall, *J. Cryst. Growth* **242**, 345 (2002).
- [26] D. Gall, I. Petrov, L. D. Madsen, J. E. Sundgren, and J. E. Greene, *J. Vac. Sci. Technol. A* **16**, 2411 (1998).
- [27] N. Takeuchi, *Phys. Rev. B* **65**, 045204 (2002).
- [28] R. Monnier, J. Rhyner, T. M. Rice and D. D. Koelling, *Phys. Rev. B* **31**, 5554 (1985).

- [29] A. Neckel, P. Rastl, R. Eibler, P. Weinberger and K. Schwarz, J. Phys. C **9**, 579 (1976).
- [30] R. Eibler, M. Dorrer and A. Neckel, Theor. Chim. Acta **63**, 133 (1983)
- [31] M. S. Abu-Jafara, A. M. Abu-Labdehb and M. El-Hasana Com. Mat. Scie. **50**, 269 (2010)
- [32] F. Tran and P. Blaha J. Phys. Chem. A **121**, 3318 (2017)
- [33] C. Stampfl, R. Asahi, and A. J. Freeman, Phys. Rev. B **65**, R161204 (2002).
- [34] A. Qteish, P. Rinke, M. Scheffler, and J. Neugebauer, Phys. Rev. B **74**, 245208 (2006).
- [35] W. R. L. Lambrecht Phys. Rev. B **62**, 13538 (2000).
- [36] P. Rinke, A. Qteish, J. Neugebauer, C. Freysold and M. Scheffler, New J. Phys. **7**, 126 (2005).
- [37] H. A. Al-Britthen, H. Yang, and A. R. Smith, J. Appl. Phys, **96**, 3787 (2004).
- [38] B. Saha, G. Naik, V. P. Drachev, A. Boltasseva, and E. Marinero, J. Appl. Phys. **114**, 063519 (2013).
- [39] C. Constantin, K. Wang, A. Chinchore, H. J. Chia, J. Markert, and A. R. Smith, Mater.Res. Soc. Symp. Proc. **1198**, E07-22 (2009).
- [40] R. Sharma and Y. Sharma, AIP Conf. Proc. **2018**, 020013 (2018).
- [41] F. Tran and P. Blaha, Phys. Rev. Lett. **102**, 226401 (2009)
- [42] V. Eyert, Int. J. Quantum Chem. **77**, 1007 (2000).
- [43] V. Eyert, The Augmented Spherical Wave Method, Lect. Notes Phys. **849** (Springer, Berlin Heidelberg 2013).
- [44] A. Houari, S.F. Matar, and M. A. Belkhir, Comp. Mat. Sci. **43**, 392 (2008).
- [45] W. Sukkabot, Physica. B: Cond. Mat. **570**, 236 (2019).
- [46] P. Hohenberg and W. Kohn, Phys. Rev. **136**, B864 (1964).
- [47] W. Kohn and L. J. Sham, Phys. Rev. **140**, A1133 (1965).
- [48] J. P. Perdew, K. Burke, and M. Ernzerhof, Phys. Rev. Lett. **77**, 3865 (1996); Phys. Rev. Lett. **78**, 1396 (1997).
- [49] A. D. Becke, J. Chem. Phys. **98**, 1372 (1993).
- [50] J. P. Perdew, M. Ernzerhof, and K. Burke, J. Chem. Phys. **105**, 9982 (1996).
- [51] C. Adamo and V. Barone, J. Chem. Phys. **110**, 6158 (1999).
- [52] J. Heyd, G. E. Scuseria, and M. Ernzerhof, J. Chem. Phys. **118**, 8207 (2003).
- [53] P. E. Blöchl, C. F. J. Walther, and T. Pruschke, Phys. Rev. B **84**, 205101 (2011).
- [54] P. E. Blöchl, T. Pruschke, and M. Potthoff, Phys. Rev. B **88**, 205139 (2013).
- [55] M. Sotoudeh, S. Rajpurohit, P. E. Blöchl, D. Mierwald, J. Norpoth, V. Roddatis, St. Mildner,

- B. Kressdorf, B. Iffland, and C. Jooss, Phys. Rev. B **95**, 235150 (2017).
- [56] M. Eckhoff, P. E. Blchl and J. Behler Phys. Rev. B **101**, 205113 (2020)
- [57] P. E. Blöchl, Phys. Rev. B **50**, 17953 (1994).
- [58] R. Car and M. Parrinello, Phys. Rev. Lett. **55**, 2471 (1985).
- [59] N. D. Mermin, Phys. Rev. **137**, A1441 (1965).
- [60] O. Jepsen and O.K. Andersen, Sol. St. Commun. **9**, 1763 (1971).
- [61] G. Lehmann and M. Taut, physica status solidi (b) **54**, 469 (1972).
- [62] P. E. Blöchl, O. Jepsen, and O. K. Andersen, Phys. Rev. B **49**, 16223 (1994).
- [63] A. Houari and F. Benissad, Adv. Theory Simul. **2**, 1900111 (2019).

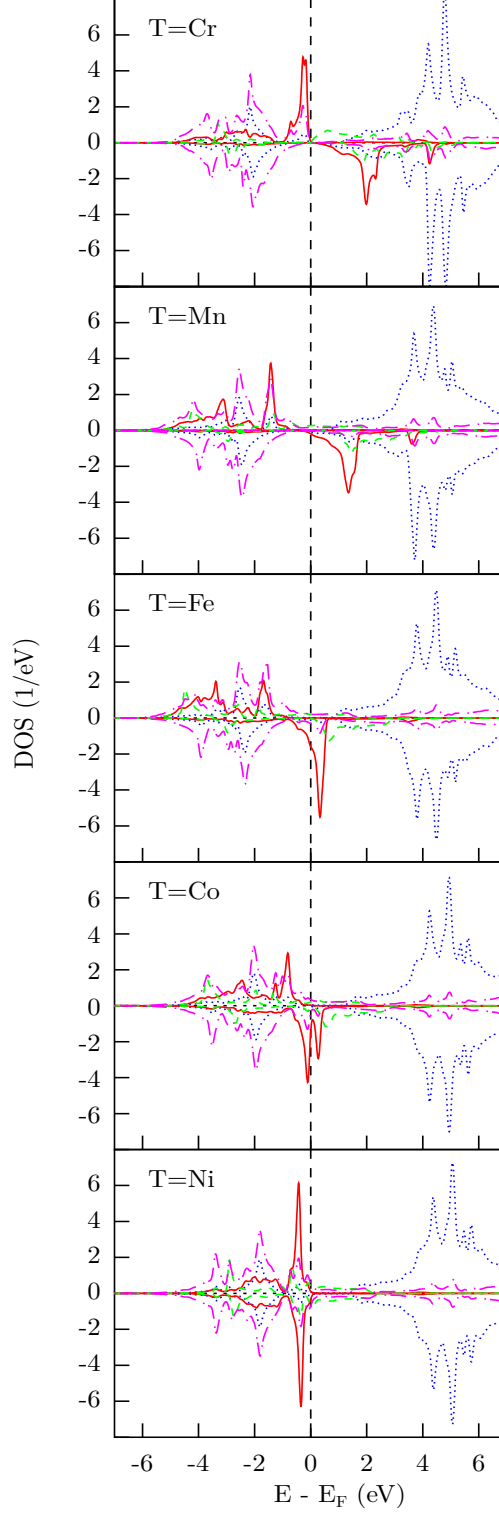


FIG. 2. (Color online) Site-, orbital-, and spin-projected density of states (DOS) of $\text{Sc}_{0.75}\text{T}_{0.25}\text{N}$ with $\text{T}=\text{Cr}$, Mn , Fe , Co , and Ni as obtained within the GGA. Sc-d , $\text{T-d-}t_{2g}$, $\text{T-d-}e_g$, and N-p contributions are given in blue (dotted), red (solid), green (dashed), and magenta (dash-dotted), respectively.

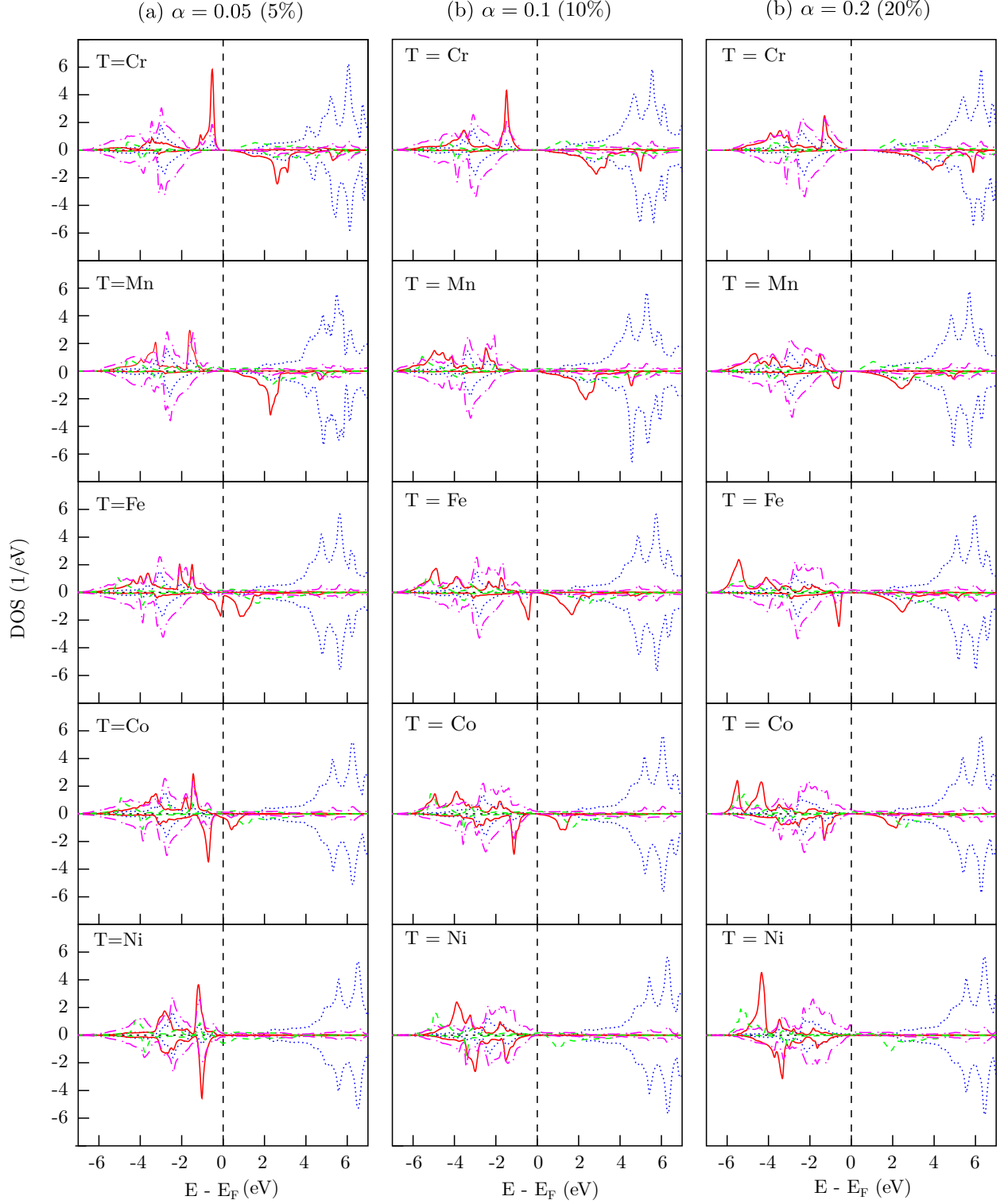


FIG. 3. (Color online) Site-, orbital-, and spin-projected density of states (DOS) of $\text{Sc}_{0.75}\text{T}_{0.25}\text{N}$ with $\text{T}=\text{Cr, Mn, Fe, Co, and Ni}$ from hybrid-functional calculations with three mixing parameters (admixture in %) of the exact exchange: $\alpha = 0.05$ (5%), $\alpha = 0.1$ (10%) and $\alpha = 0.2$ (20%). The Sc- d , T- $d-t_{2g}$, T- $d-e_g$, and N- p contributions (color and lines) are the same as in Fig. 2.

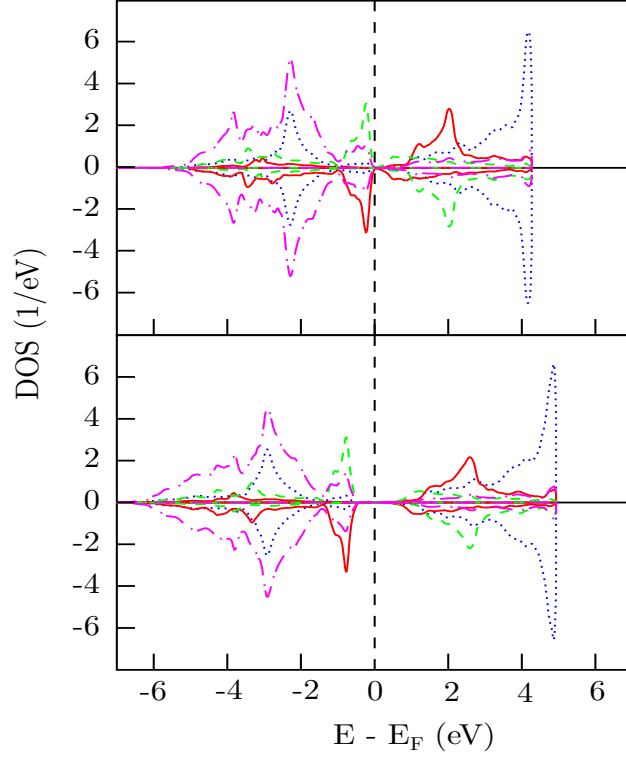


FIG. 4. (Color online) Site-, orbital-, and spin-projected density of states (DOS) of antiferromagnetic $\text{Sc}_{0.75}\text{Cr}_{0.25}\text{N}$ as obtained from GGA calculations (top) and hybrid-functional calculations (bottom). Sc- d and N- p contributions are given in blue (dotted) and magenta (dash-dotted), respectively, while the contributions of the Cr- d states of the two sublattices are given in red (solid) and (green) (dashed).

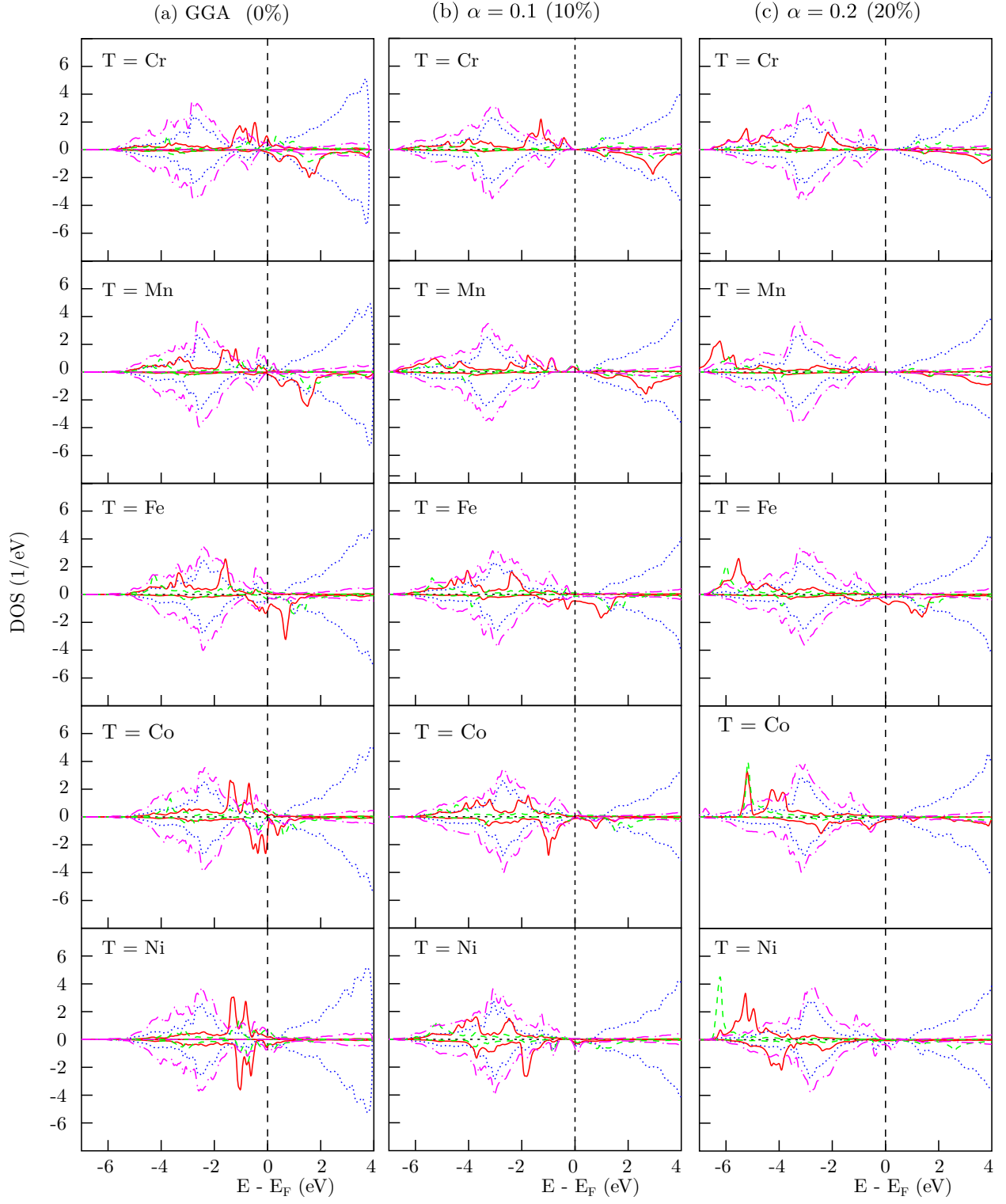


FIG. 5. (Color online) Site-, orbital-, and spin-projected density of states (DOS) of $\text{Sc}_{0.9}\text{T}_{0.1}\text{N}$ with $\text{T}=\text{Cr, Mn, Fe, Co, and Ni}$ obtained from GGA as well as hybrid-functional with $\alpha=0.1$ and $\alpha=0.2$. The contributions of the atomic species (lines and colors) are the same as in Fig. 3.